RESEARCH PAPERS

Piotr Rᴀᴘᴘ

COMPUTATIONAL MODEL OF ADHESIVE SCARF JOINTS IN TIMBER BEAMS

The subject of this paper is the general formulation of a model for scarf adhesive joints in timber beams within the framework of plane linear elasticity. It is assumed that wood is orthotropic. The joint can be subjected to a complex loading state including an axial force, a bending moment and a shear force. The joint model is given in displacements by means of a set of four partial differential equations of the second order. Boundary conditions cater for sharp edges in the adherends. Complete solutions to theory of elasticity equations are presented and discussed. The manner in which the joint transmits the axial force, the bending moment and the shear force is presented. It is shown that the scarf joint does not feature stress concentrations and that there exists an approximate equivalence of displacements and stress states in scarf jointed and continuous elements.

Keywords: timber beam, adhesive scarf joint, analytical model, two dimensional displacement-stress analysis, orthotropy, linear elasticity

Introduction

The repair of timber structures including beams is of practical importance in civil engineering. An example of this would be the replacement of a biologically-corroded, damaged end section of a floor beam or a rafter. Simple methods, such as when a new fragment is joined with the old beam by various types of wooden plates or steel profiles, have been in use for some time. They are effective but usually lead to a change in the external look of the elements, changes in the static scheme and application of the materials which differ from the original ones. Such solutions are not acceptable in historical structures, where not only are the

———————
     Piotr Rᴀᴘᴘ (*piotr.rapp@put.poznan.pl, piotrrapp@gmail.com*), Poznan University of Technology, Poznan, Poland

architecture and decoration of great value, but also the structure itself. In such cases, the shapes, the appearance of the structural elements, the static schemes, materials, etc. must be preserved.

One possible solution allowing for the repair of a damaged element, while preserving its original shape, appearance, material, strength, and static scheme, is the use of an adhesive scarf joint (fig. 1).
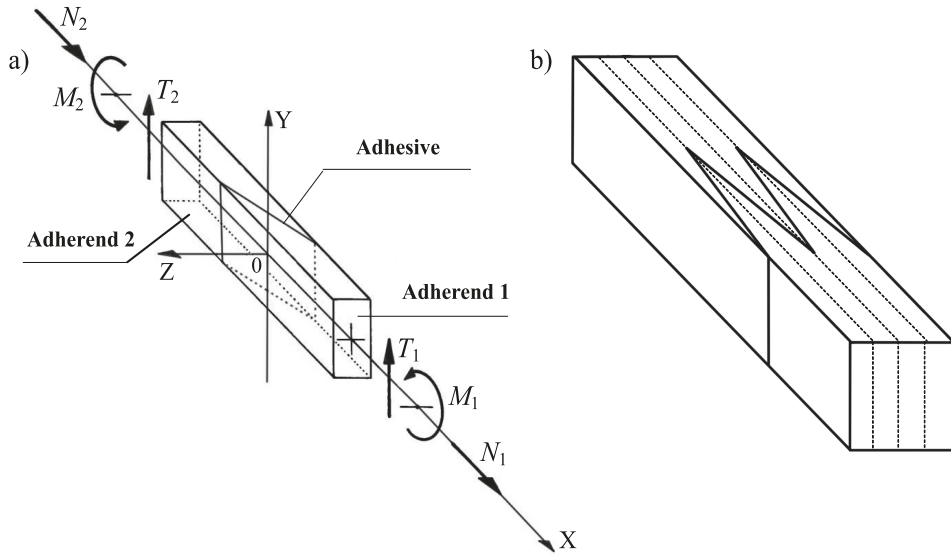

Fig. 1. Adhesive scarf joints in wooden beams: a) scarf joint and its loading, b) scarf joints in a wide beam

It is important that in the considered joint the adhesive plane is parallel to the Y axis lying in the beam bending plane 0XY (fig. 1a). In a wide beam, a single scarf joint would be too long, therefore multiple joints can be used to keep them small – see fig. 1b. In such a case, it is assumed that the wide beam consists of several narrower segments with single scarf joints and each segment transmits an appropriate part of loading.

These types of joints are rarely used in wooden beam structures and, as technological solutions, they do not yet possess complete theoretical or experimental documentation.

In other cases, differing from the ones described in this paper, scarf joints are frequently used under axial tension [Erdogan, Ratawani 1971; Reddy, Sinha 1975] or in beams under bending as joints in the form of micro-dovetails (finger joints), where the joint is perpendicular to the bending plane [Tomasiuk 1988; Smardzewski 1996].

In this paper, the general results previously presented by Rapp are used [2010a, 2010b].

The adhesive scarf joint model

A timber beam with a rectangular cross-section consisting of two elements with thickness values g_1 and g_2 is considered. In general, various wood types may be used. The adherends are connected by an adhesive scarf joint. A set of co-ordinates 0XYZ is associated with the beam. The plane 0XY represents the bending plane, according to fig. 1. The adhesive is a plane rectangle forming the angle φ_x with the bending plane 0XY. The adhesive projection on the plane 0XY is the rectangle ABCD with dimensions $2l_x \times 2l_y$ (fig. 2).
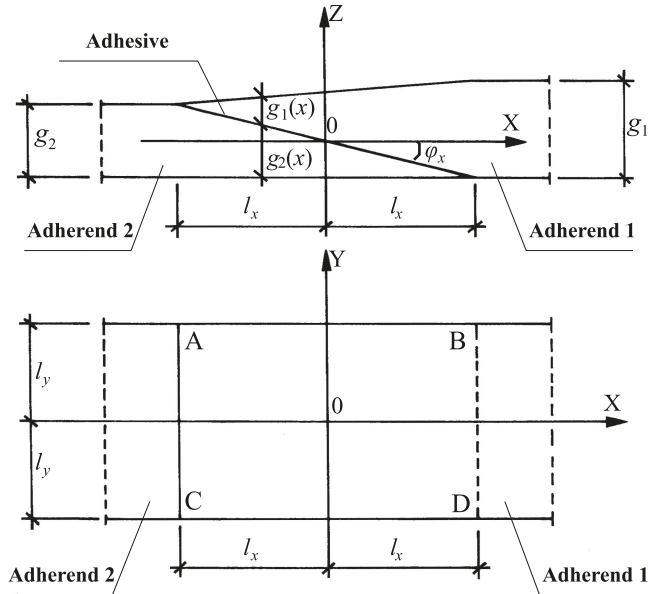

Fig. 2. The adhesive scarf joint model

It is assumed that stresses across the adherend thickness are constant and form plane stress states parallel to the plane 0XY. Hence, the adherends are considered as plane stress elements parallel to the plane 0XY. The adherend thickness is measured in the direction normal to the plane 0XY. In the joint zone, the adherend thickness values $g_1(x)$ and $g_2(x)$ vary linearly from zero to g_1 and g_2 along the X axis and are constant along the Y axis.

$$g_1(x) = \frac{g_1}{2l_x}x + \frac{g_1}{2}, \ g_2(x) = -\frac{g_2}{2l_x}x + \frac{g_2}{2} \tag{1}$$

The adhesive thickness t is measured in the direction normal to its plane.

The adhesive is modelled as an isotropic linearly-elastic medium with Young's modulus E_s, the shear modulus G_s and Poisson's ratio v_s, where $E_s = 2(1 + v_s)G_s$.

Stresses in the adhesive are defined as interactions between adherend 1 and the adhesive. There are shear stresses $\tau_x = \tau_x(x, y)$ and $\tau_y = \tau_y(x, y)$ in the adhesive plane and the stress $\sigma_N = \sigma_N(x, y)$ normal to the adhesive plane. The stress τ_x is parallel to the plane 0XZ, and the stress τ_y is parallel to the Y axis (fig. 3).
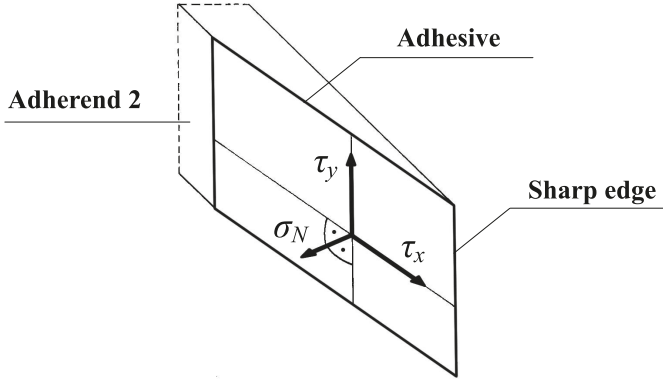

Fig. 3. Stresses in the adhesive

It is assumed that the stresses in the adhesive are constant across its thickness. The stresses presented in fig. 3 are positive. Due to the action of the shear stresses τ_x and τ_y, a shear deformation in the adhesive occurs. This leads to relative displacements of layers in the adhesive in the direction parallel to the adhesive plane. The stress σ_N leads to axial strains normal to the adhesive plane.

The displacements in adherends 1 and 2 of the scarf joint are defined by the functions $u_1 = u_1(x, y)$ and $u_2 = u_2(x, y)$ along the X axis and the functions $v_1 = v_1(x, y)$ and $v_2 = v_2(x, y)$ along the Y axis. The displacements u_1, u_2, v_1, and v_2 are positive when they coincide with the positive orientation of the X and Y axes. It is assumed that the functions u_1, u_2, v_1, and v_2 are C^2 – continuous with respect to variables x and y.

In the following, the functions of the displacements u_1, u_2, v_1, and v_2 are considered as unknowns and all the quantities related to the adhesive joint are expressed in their terms.

The loading of the adhesive joint can be represented by forces parallel to the plane 0XY distributed along the edges of the adherends. The loading is positive when its orientation coincides with the positive orientation of the X and Y axes.

There are axial forces, bending moments and shear forces in the beam cross-sections. They lead to the axial stresses p_{1x} and p_{2x} distributed linearly, and the shear stresses p_{1y} and p_{2y} with a parabolic distribution. Hence, it is assumed that the edges of the adherends can be loaded by axial forces, bending moments and shear forces. The positive orientation of these forces and the corresponding stress distributions are presented in fig. 4. The joint loading must remain in equilibrium.
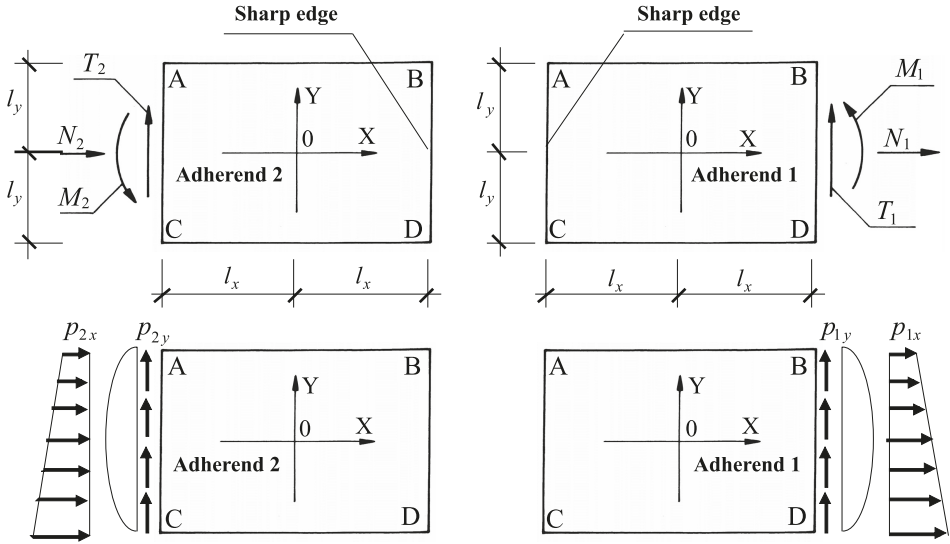
Fig. 4. Loading of the scarf joint adherends

Constitutive equations for the adherends

It is assumed that generally the adherends are made of different wood types, both orthotropic, and that the main axes of orthotropy coincide with the X and Y axes. In the plane stress state, the constitutive relations for adherends 1 and 2 are given by:

$$\varepsilon_{kx} = \frac{1}{E_{kx}}\sigma_{kx} - \frac{v_{kxy}}{E_{ky}}\sigma_{ky} \tag{2}$$

$$\varepsilon_{ky} = -\frac{v_{kyx}}{E_{kx}}\sigma_{kx} + \frac{1}{E_{ky}}\sigma_{ky} \tag{3}$$

$$\gamma_{kxy} = \frac{1}{G_{kxy}}\tau_{kxy} \tag{4}$$

where: $k = 1$ for adherend 1 and $k = 2$ for adherend 2.

An orthotropic material in the plane stress state is described by five material constants: two coefficients of longitudinal elasticity E_{kx} and E_{ky} one shear modulus of the set of equations (2) – (3) is symmetric, i.e. G_{kxy}, and two Poisson's ratios v_{kxy} and v_{kyx}. It is assumed that the matrix of coefficients:

$$\frac{v_{kyx}}{E_{kx}} = \frac{v_{kxy}}{E_{ky}} \tag{5}$$

holds. Thus, four out of five material parameters are independent.

Having solved the set of equations (2) – (4) with respect to stresses, one gets:

$$\sigma_{kx} = \frac{E_{kx}}{1 - v_{kxy}v_{kyx}} \varepsilon_{kx} + \frac{v_{kxy}E_{kx}}{1 - v_{kxy}v_{kyx}} \varepsilon_{ky} \tag{6}$$

$$\sigma_{ky} = \frac{v_{kyx}E_{ky}}{1 - v_{kxy}v_{kyx}} \varepsilon_{kx} + \frac{E_{ky}}{1 - v_{kxy}v_{kyx}} \varepsilon_{ky} \tag{7}$$

$$\tau_{kxy} = G_{kxy}\gamma_{kxy} \tag{8}$$

where: $k = 1$ for adherend 1 and $k = 2$ for adherend 2.

The material parameters E_{kx} E_{ky} G_{kxy}, v_{kxy} and v_{kyx} should be assumed to be dependent on the annular ring orientation in the beam cross-section. In the tree trunk model consisting of concentric annular rings, three anatomic directions are defined: parallel to the grains L, radial R and transverse T (fig. 5a). The mechanical properties of wood differ in these anatomic directions. At every point of the trunk model, the L, R, T axes are mutually orthogonal and can be treated as the local set of principal axes of orthotropy.
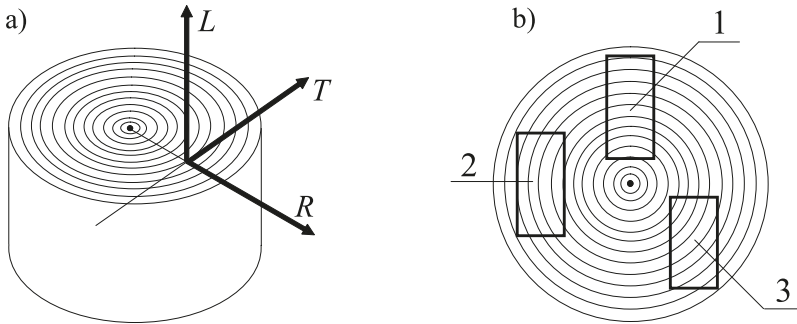

Fig. 5. Anisotropy of wood: a) the trunk model, b) particular cases of beam cross-section location in the trunk model

At an arbitrary point in the trunk model, the constitutive relations take the form:

$$\varepsilon_L = \frac{1}{E_L}\sigma_L - \frac{v_{LR}}{E_R}\sigma_R - \frac{v_{LT}}{E_T}\sigma_T \tag{9}$$

$$\varepsilon_R = -\frac{v_{RL}}{E_L}\sigma_L + \frac{1}{E_R}\sigma_R - \frac{v_{RT}}{E_T}\sigma_T \qquad (10)$$

$$\varepsilon_T = -\frac{v_{TL}}{E_L}\sigma_L - \frac{v_{TR}}{E_R}\sigma_R + \frac{1}{E_T}\sigma_T \qquad (11)$$

$$\gamma_{LR} = \frac{1}{G_{LR}}\tau_{LR} \qquad (12)$$

$$\gamma_{LT} = \frac{1}{G_{LT}}\tau_{LT} \qquad (13)$$

$$\gamma_{RT} = \frac{1}{G_{RT}}\tau_{RT} \qquad (14)$$

Examples of material constants for some types of wood determined experimentally are presented in [Keylwerth 1951; Goodman, Bodig 1970; Neuhaus 1994].

If the beam bending plane coincides with the radial direction (cross-section 1 in fig. 5b) then it may be assumed that the beam orthotropy in the bending plane is defined by the L and R axes. In this case, the material constants in the equations (2) – (3) are $E_{kx} = E_L$, $E_{ky} = E_R$, $G_{kxy} = G_{LR}$, $v_{kxy} = v_{LR}$, and $v_{kyx} = v_{RL}$. If the coefficient matrix of the set of equations (2) – (3) is not symmetric, then it can be symmetrised by an approximate assumption that $v_{kxy} = v_{RL}(E_R/E_L)$.

If the beam bending plane coincides with the transverse direction (cross-section 2 in fig. 5b), then it may be assumed that the beam orthotropy in the bending plane is defined by the L and T axes. In this case, the material constants in the equations (2) – (3) are $E_{kx} = E_L$, $E_{ky} = E_T$, $G_{kxy} = G_{LT}$, $v_{kxy} = v_{LT}$, and $v_{kyx} = v_{TL}$. If the coefficient matrix of the set of equations (2) – (3) is not symmetric, then it can be symmetrised by an approximate assumption that $v_{kxy} = v_{TL}(E_T/E_L)$.

If the beam bending plane is not parallel to either of the R or T axes (cross-section 3 in fig. 5b), then it can be assumed that the wood can be modelled by a composite with a transverse isotropy. Then the direction L parallel to the grain is assumed, and the directions in the cross-sections perpendicular to the L axis are unified. In reality, this is the most frequent case. Transversely isotropic elements subjected to a plane stress state can be described using the elasticity moduli $E_{0,mean}$, $E_{90,mean}$, and G_{mean} introduced in Eurocode 5, where $E_{0,mean}$ – the mean elasticity modulus along the grain, $E_{90,mean}$ – the mean elasticity modulus across the grain and G_{mean} – the mean shear modulus. It is assumed that $E_{kx} = E_{k,0,mean}$, $E_{ky} = E_{k,90,mean}$, and $G_{kxy} = G_{k,mean}$ in the equations (2) – (4).

For coniferous wood, $v_{TL} = v_{RL} = v_{kyx} = 0.45$, approximately. From the relation $E_{k,90, mean} = E_{k,0, mean}/30$ and the symmetry condition (5) $v_{kxy} = 0.015$ can be determined ($k = 1$ for adherend 1 and $k = 2$ for adherend 2).

Taking into account the Cauchy geometric relations:

$$\varepsilon_{kx} = \frac{\partial u_k}{\partial x}, \quad \varepsilon_{ky} = \frac{\partial v_k}{\partial y}, \quad \gamma_{kxy} = \frac{\partial u_k}{\partial y} + \frac{\partial v_k}{\partial x} \tag{15}$$

the constitutive equations (6) – (8) for adherends 1 and 2 can be given in the form:

$$\sigma_{kx} = \frac{E_{kx}}{1 - v_{kxy}v_{kyx}}\frac{\partial u_k}{\partial x} + \frac{v_{kxy}E_{kx}}{1 - v_{kxy}v_{kyx}}\frac{\partial v_k}{\partial y} \tag{16}$$

$$\sigma_{ky} = \frac{v_{kyx}E_{ky}}{1 - v_{kxy}v_{kyx}}\frac{\partial u_k}{\partial x} + \frac{E_{ky}}{1 - v_{kxy}v_{kyx}}\frac{\partial v_k}{\partial y} \tag{17}$$

$$\tau_{kxy} = G_{kxy}\left(\frac{\partial u_k}{\partial y} + \frac{\partial v_k}{\partial x}\right) \tag{18}$$

where: $k = 1$ for adherend 1 and $k = 2$ for adherend 2.

Constitutive equations for the adhesive

Stresses in the adhesive are due to differences between displacements of adherends 1 and 2. From the general considerations presented by Rapp [2010a, 2010b], relations between the stresses in the adhesive and the displacements of the adherends for a scarf joint can be written in the form:

$$\tau_x = \frac{E_s G_s}{t(E_s + G_s \mathrm{tg}^2 \varphi_x)\cos\varphi_x}(u_1 - u_2) \tag{19}$$

$$\tau_y = \frac{G_s}{t}(v_1 - v_2) \tag{20}$$

$$\sigma_N = \tau_x \mathrm{tg}\varphi_x \tag{21}$$

Displacement equations and boundary conditions

A general formulation of the displacement equations and the boundary conditions for two-dimensional adhesive joints was presented by Rapp [2010a, 2010b]. For an adhesive scarf joint they take the form:

$$\left(\alpha_{1x}\frac{\partial^2 u_1}{\partial x^2}+\frac{\partial^2 u_1}{\partial y^2}+\beta_{1x}\frac{\partial^2 \upsilon_1}{\partial x\partial y}\right)\left(\frac{g_1}{2l_x}x+\frac{g_1}{2}\right)+\left(\alpha_{1x}\frac{\partial u_1}{\partial x}+(\beta_{1x}-1)\frac{\partial \upsilon_1}{\partial y}\right)\frac{g_1}{2l_x}-\gamma_{1u}(u_1-u_2)=0 \quad (22)$$

$$\left(\frac{\partial^2 \upsilon_1}{\partial x^2}+\alpha_{1y}\frac{\partial^2 \upsilon_1}{\partial y^2}+\beta_{1y}\frac{\partial^2 u_1}{\partial x\partial y}\right)\left(\frac{g_1}{2l_x}x+\frac{g_1}{2}\right)+\left(\frac{\partial u_1}{\partial y}+\frac{\partial \upsilon_1}{\partial x}\right)\frac{g_1}{2l_x}-\gamma_{1\upsilon}(\upsilon_1-\upsilon_2)=0 \quad (23)$$

$$\left(\alpha_{2x}\frac{\partial^2 u_2}{\partial x^2}+\frac{\partial^2 u_2}{\partial y^2}+\beta_{2x}\frac{\partial^2 \upsilon_2}{\partial x\partial y}\right)\left(-\frac{g_2}{2l_x}x+\frac{g_2}{2}\right)-\left(\alpha_{2x}\frac{\partial u_2}{\partial x}+(\beta_{2x}-1)\frac{\partial \upsilon_2}{\partial y}\right)\frac{g_2}{2l_x}+\gamma_{2u}(u_1-u_2)=0 \quad (24)$$

$$\left(\frac{\partial^2 \upsilon_2}{\partial x^2}+\alpha_{2y}\frac{\partial^2 \upsilon_2}{\partial y^2}+\beta_{2y}\frac{\partial^2 u_2}{\partial x\partial y}\right)\left(-\frac{g_2}{2l_x}x+\frac{g_2}{2}\right)-\left(\frac{\partial u_2}{\partial y}+\frac{\partial \upsilon_2}{\partial x}\right)\frac{g_2}{2l_x}+\gamma_{2\upsilon}(\upsilon_1-\upsilon_2)=0 \quad (25)$$

where:

$$\alpha_{kx}=\frac{E_{kx}}{G_{kxy}(1-\nu_{kxy}\nu_{kyx})},\ \alpha_{ky}=\frac{E_{ky}}{G_{kxy}(1-\nu_{kxy}\nu_{kyx})} \tag{26}$$

$$\beta_{kx}=1+\frac{\nu_{kxy}E_{kx}}{G_{kxy}(1-\nu_{kxy}\nu_{kyx})}=1+\alpha_{kx}\nu_{kxy},\ \beta_{ky}=1+\frac{\nu_{kyx}E_{ky}}{G_{kxy}(1-\nu_{kxy}\nu_{kyx})}=1+\alpha_{ky}\nu_{kyx} \tag{27}$$

$$\gamma_{ku}=\frac{E_s G_s}{t\,G_{kxy}(E_s+G_s\mathrm{tg}^2\varphi_x)\cos^3\varphi_x},\ \ \gamma_{k\upsilon}=\frac{G_s}{t\,G_{kxy}\cos\varphi_x} \tag{28}$$

where: $k=1$ for adherend 1 and $k=2$ for adherend 2.

The equations (22) – (25) represent a set of four elliptic partial differential equations of the second order, with varying coefficients where the displacement functions u_1, u_2, υ_1, and υ_2 for adherends 1 and 2 are unknown. From condition (5) and formulae (27) one gets $\beta_{kx}=\beta_{ky}$.

There is a normal loading p_{1x} and a shear loading p_{1y} acting on the edge $x=l_x$ of adherend 1, while on the edge $x=-l_x$ of adherend 2 – a normal loading p_{2x} and a shear loading p_{2y} are found (fig. 4). The edges: $x=-l_x$ for adherend 1 and $x=l_x$ for adherend 2 have zero thickness and are called sharp edges (fig. 3). The remaining edges are non-sharp.

The boundary conditions for non-sharp edges read:
  – adherend 1, the edge $x=l_x$:

$$\alpha_{1x}\frac{\partial u_1}{\partial x}+(\beta_{1x}-1)\frac{\partial \upsilon_1}{\partial y}=\frac{p_{1x}}{G_{1xy}},\ \ \frac{\partial u_1}{\partial y}+\frac{\partial \upsilon_1}{\partial x}=\frac{p_{1y}}{G_{1xy}} \tag{29}$$

– adherend 1, the edge $y = \pm l_y$:

$$(\beta_{1y} - 1)\frac{\partial u_1}{\partial x} + \alpha_{1y}\frac{\partial v_1}{\partial y} = 0, \quad \frac{\partial u_1}{\partial y} + \frac{\partial v_1}{\partial x} = 0 \tag{30}$$

– adherend 2, the edge $x = -l_x$:

$$\alpha_{2x}\frac{\partial u_2}{\partial x} + (\beta_{2x} - 1)\frac{\partial v_2}{\partial y} = -\frac{p_{2x}}{G_{2xy}}, \quad \frac{\partial u_2}{\partial y} + \frac{\partial v_2}{\partial x} = -\frac{p_{2y}}{G_{2xy}} \tag{31}$$

– adherend 2, the edge $y = \pm l_y$:

$$(\beta_{2y} - 1)\frac{\partial u_2}{\partial x} + \alpha_{2y}\frac{\partial v_2}{\partial y} = 0, \quad \frac{\partial u_2}{\partial y} + \frac{\partial v_2}{\partial x} = 0 \tag{32}$$

For the sharp edges, we get:
– adherend 1, the edge $x = -l_x$:

$$\left(\alpha_{1x}\frac{\partial u_1}{\partial x} + (\beta_{1x} - 1)\frac{\partial v_1}{\partial y}\right)\frac{g_1}{2l_x} - \gamma_{1u}(u_1 - u_2) = 0 \tag{33}$$

$$\left(\frac{\partial u_1}{\partial y} + \frac{\partial v_1}{\partial x}\right)\frac{g_1}{2l_x} - \gamma_{1v}(v_1 - v_2) = 0 \tag{34}$$

– adherend 2, the edge $x = l_x$:

$$\left(\alpha_{2x}\frac{\partial u_2}{\partial x} + (\beta_{2x} - 1)\frac{\partial v_2}{\partial y}\right)\frac{g_2}{2l_x} - \gamma_{2u}(u_1 - u_2) = 0 \tag{35}$$

$$\left(\frac{\partial u_2}{\partial y} + \frac{\partial v_2}{\partial x}\right)\frac{g_2}{2l_x} - \gamma_{2v}(v_1 - v_2) = 0 \tag{36}$$

In order to ensure the uniqueness of the solution to the boundary value problem, one should define in the displacement formulation, besides the static conditions, the kinematic boundary conditions to constrain movement of the joint.

The boundary value problem (22) – (25), (29) – (36) is solved using the finite difference method. The finite difference mesh within the rectangle $2l_x \times 2l_y$ covering the projection of the adhesive joint on the plane 0XY is shown in fig. 6.
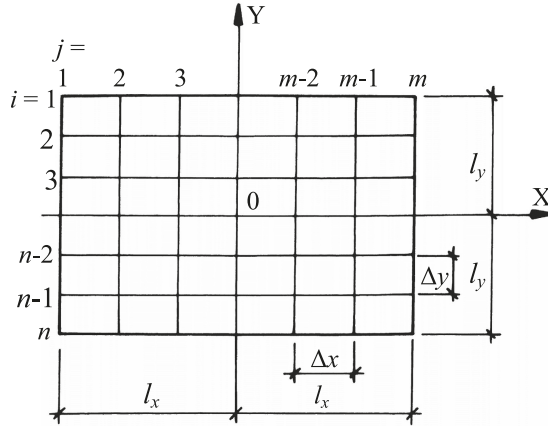
Fig. 6. The finite difference mesh on the projection of the adhesive joint

The finite difference mesh has a regular rectangular shape with the side lengths Δx and Δy. There are m nodes along the X axis ($j = 1, 2, ..., m$), and n nodes along the Y axis ($i = 1, 2, ..., n$), while $n, m \geq 5$. It is assumed that n and m are odd numbers. The unknown parameters in the finite difference method are the displacements $u_{ki,j}$ and $v_{ki,j}$ at the nodes of the mesh.

Having determined the displacements u_1, u_2, v_1, and v_2, one can calculate the stresses in the adherends using the formulae (6) – (8). The stresses τ_x, τ_x and σ_N in the adhesive follow from (19) – (21).

A scarf joint loaded axially

Let us now consider an adhesive scarf joint between the adherends with dimensions $l_x = 22.5$ cm, $l_y = 10.25$ cm, $g_1 = g_2 = g = 4.5$ cm made of identical wood with the following properties:

$$E_{1x} = E_{2x} = E_x = 1.2 \cdot 10^6 \text{ N/cm}^2, E_{1y} = E_{2y} = E_y = 0.8 \cdot 10^5 \text{ N/cm}^2$$

$$G_{1xy} = G_{2xy} = G_{xy} = 0.6 \cdot 10^5 \text{ N/cm}^2, v_{1xy} = v_{2xy} = v_{xy} = 0.03, v_{1yx} = v_{2yx} = v_{yx} = 0.45$$

The adhesive has the thickness $t = 0.05$ cm and the material constants:

$$E_s = 1.215 \cdot 10^5 \text{ N/cm}^2, G_s = 0.45 \cdot 10^5 \text{ N/cm}^2, v_s = 0.35$$

The joint is subjected to the tensile forces $N_1 = - N_2 = 1$ N. Thus, the edges: $x = l_x$ for adherend 1 and $x = - l_x$ for adherend 2 are under the action of the uniformly distributed stresses: $p_{1x} = 0.(01084)$ N/cm² and $p_{2x} = - 0.(01084)$ N/cm², respectively. The problem is solved using the finite difference method with the mesh $n \times m = 21 \times 45$ ($\Delta x = 1.02(27)$ cm, $\Delta y = 1.025$ cm). The kinematic boundary conditions introduced for adherend 1 as the constraint of the node $(i, j) = (11, 23)$ in the direction of the X axis and the nodes $(i, j) = (11, 13), (11, 33)$ in the direction of the Y axis.

The displacements of the adherends at selected nodes of the finite difference mesh are given in table 1.

Table 1. The displacements of the adherends in a scarf joint loaded axially [cm]

		Displacements of adherend 1				Displacements of adherend 2		
	$i\backslash j$	1	23	45		1	23	45
u_1	1	$-2.0325 \cdot 10^{-7}$	0	$2.0325 \cdot 10^{-7}$	u_2	$-2.0444 \cdot 10^{-7}$	$-1.1910 \cdot 10^{-9}$	$2.0206 \cdot 10^{-7}$
v_1		$-4.1667 \cdot 10^{-8}$	$-4.1667 \cdot 10^{-8}$	$-4.1667 \cdot 10^{-8}$	v_2	$-4.1667 \cdot 10^{-8}$	$-4.1667 \cdot 10^{-8}$	$-4.1667 \cdot 10^{-8}$
u_1	11	$-2.0325 \cdot 10^{-7}$	0	$2.0325 \cdot 10^{-7}$	u_2	$-2.0444 \cdot 10^{-7}$	$-1.1910 \cdot 10^{-9}$	$2.0206 \cdot 10^{-7}$
v_1		0	0	0	v_2	0	0	0
u_1	21	$-2.0325 \cdot 10^{-7}$	0	$2.0325 \cdot 10^{-7}$	u_2	$-2.0444 \cdot 10^{-7}$	$-1.1910 \cdot 10^{-9}$	$2.0206 \cdot 10^{-7}$
v_1		$4.1667 \cdot 10^{-8}$	$4.1667 \cdot 10^{-8}$	$4.1667 \cdot 10^{-8}$	v_2	$4.1667 \cdot 10^{-8}$	$4.1667 \cdot 10^{-8}$	$4.1667 \cdot 10^{-8}$

The distributions of displacement functions u_1, u_2 and v_1, v_2 for the adherends are given in fig. 7. The displacements for both adherends are depicted in single drawings, because with the adopted scale, the differences between the appropriate displacement values are indistinguishable.
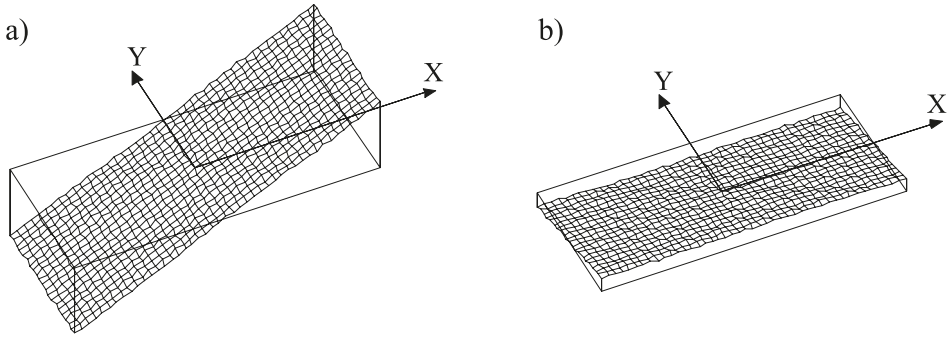
Fig. 7. The displacements in the adherends of an axially loaded scarf joint: a) displacements u_1, u_2, b) displacements v_1, v_2

The remaining results of the calculations are:
- the shear stresses τ_x and τ_y in the adhesive:

$$\tau_x = 1.0733 \cdot 10^{-3} \text{ N/cm}^2 = \text{const}, \quad \tau_y = 0 \text{ N/cm}^2$$

- the normal stress σ_N in the adhesive (fig. 10):

$$\sigma_N = 1.0733 \cdot 10^{-4} \text{ N/cm}^2 = \text{const}$$

- the normal stresses σ_{1x}, σ_{1y} and the shear stress τ_{1xy} in adherend 1:

$$\sigma_{1x} = 1.0840 \cdot 10^{-2} \text{ N/cm}^2 = \text{const}, \quad \sigma_{1y} = 0 \text{ N/cm}^2, \quad \tau_{1xy} = 0 \text{ N/cm}^2$$

– the normal stresses σ_{2x}, σ_{2y} and the shear stress τ_{2xy} in adherend 2:

$$\sigma_{2x} = 1.0840 \cdot 10^{-2} \text{ N/cm}^2 = \text{const}, \; \sigma_{2y} = 0 \text{ N/cm}^2, \; \tau_{2xy} = 0 \text{ N/cm}^2$$

The solution presented to the two-dimensional problem in the theory of elasticity may be verified using a model of a one-dimensional axially loaded rod. Using the semi-inverse method of the theory of elasticity, one can define the displacements u_1, u_2, v_1, and v_2 of the adherends with the following formulae:

$$u_1(x,y) = \frac{p_{1x}}{E_x} x + \frac{tg(E_s + G_s tg^2 \varphi_x) \cos^3 \varphi_x}{2 l_x G_s E_s} p_{1x} + Ay + B \tag{38}$$

$$u_2(x,y) = \frac{p_{1x}}{E_x} x + Ay + B \tag{39}$$

$$v_1(x,y) = v_2(x,y) = -\frac{v_{yx} p_{1x}}{E_x} y - Ax + C \tag{40}$$

where: A, B and C are arbitrary constants to be derived from kinematic boundary conditions.

A simple substitution makes it possible to check that the functions (38) – (40) fulfill the equations (22) – (25) and the boundary conditions (29) – (36) with the constants E_x, E_y, G_{xy}, v_{xy}, and v_{yx} for both adherends, as well as the equilibrium condition for the loading $p_{1x} + p_{2x} = 0$.

Having substituted the relations (38) – (40) to the formulae (16) – (18), the stresses in the adherends can be found as:

$$\sigma_{1x}(x,y) = \sigma_{2x}(x,y) = p_{1x} = \text{const} \tag{41}$$

$$\sigma_{1y}(x,y) = \sigma_{2y}(x,y) = 0 \tag{42}$$

$$\tau_{1xy}(x,y) = \tau_{2xy}(x,y) = 0 \tag{43}$$

Knowing the displacement functions (38) – (40), one can determine the stresses in the adhesive τ_x, τ_y and σ_N using (19) – (21):

$$\tau_x(x,y) = p_{1x} \sin \varphi_x \cos \varphi_x = \text{const} \tag{44}$$

$$\tau_y(x,y) = 0 \tag{45}$$

$$\sigma_N(x,y) = p_{1x} \sin^2 \varphi_x = \text{const} \tag{46}$$

The kinematic boundary conditions yield the zero constants A and C present in the equations (38) – (40), while the constant B is given by:

$$B = -\frac{tg(E_s + G_s tg^2\varphi_x)\cos^3\varphi_x}{2l_x G_s E_s}p_{1x} \tag{47}$$

The displacement functions for the adherends are given by:

$$u_1(x,y) = \frac{p_{1x}}{E_x}x \tag{48}$$

$$u_2(x,y) = \frac{p_{1x}}{E_x}x - \frac{tg(E_s + G_s tg^2\varphi_x)\cos^3\varphi_x}{2l_x G_s E_s}p_{1x} \tag{49}$$

$$\upsilon_1(x,y) = \upsilon_2(x,y) = -\frac{v_{yx}p_{1x}}{E_x}y \tag{50}$$

The functions (48) – (50) fulfill the equations (22) – (25), the static boundary conditions (29) – (36) and the kinematic boundary conditions. The uniqueness of the solution for the theory of elasticity problem makes it possible to conclude that the functions (48) – (50) are solutions to the two-dimensional problem of the scarf joint.

The stress state in the adherends and the adhesive, in the case of a scarf joint loaded axially with two adherends made of an identical material, does not depend on the adhesive thickness and its material parameters. Additionally, the stresses are identical to those in a skew section at the angle $\ddot{o}_x$ in a one-dimensional continuous element, under a uniaxial stress state.

The adhesive parameters influence only the difference between the displacements of adherends 1 and 2, which is evident in formulae (48) and (49).

The equivalence of the one- and two-dimensional models, and the independence of values and distributions of stresses with respect to the adhesive parameters, do not occur in the case of a joint between adherends made from different materials, for a different loading than a uniform axial one or when $g_1 \neq g_2$.

For instance, let us look at a scarf joint loaded axially but located between two adherends made from different materials with the following parameters:

$$E_{1x} = 1.2 \cdot 10^6 \text{ N/cm}^2, \ E_{1y} = 0.8 \cdot 10^5 \text{ N/cm}^2, \ G_{1xy} = 0.6 \cdot 10^5 \text{ N/cm}^2$$
$$v_{1xy} = 0.03, \ v_{1yx} = 0.45$$
$$E_{2x} = 0.9 \cdot 10^6 \text{ N/cm}^2, \ E_{2y} = 0.45 \cdot 10^5 \text{ N/cm}^2, \ G_{2xy} = 0.5 \cdot 10^5 \text{ N/cm}^2$$
$$v_{2xy} = 0.018, \ v_{2yx} = 0.36$$

All the other data remain the same as in the case considered previously.

Two-dimensional stress and displacement states are present in the adhesive and the adherends. To illustrate the problem, figs. 8–10 present the distributions of displacements and stresses in the adherends and in the adhesive. Note, that figs. 9 c–f and 10 have a different scale to figs. 9 a, b.

The displacements u_1, u_2 and v_1, v_2 in fig. 8 for both adherends are depicted in single drawings, because with the adopted scale, the differences between the appropriate displacement values are indistinguishable.
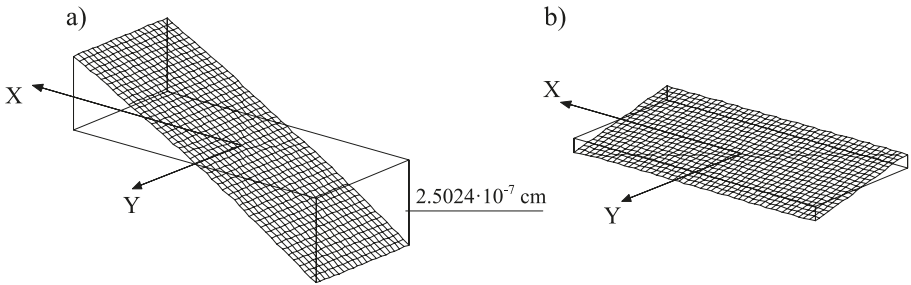
Fig. 8. The displacements in the adherends of a scarf joint loaded axially in the case of different materials: a) displacements u_1, u_2, b) displacements v_1, v_2
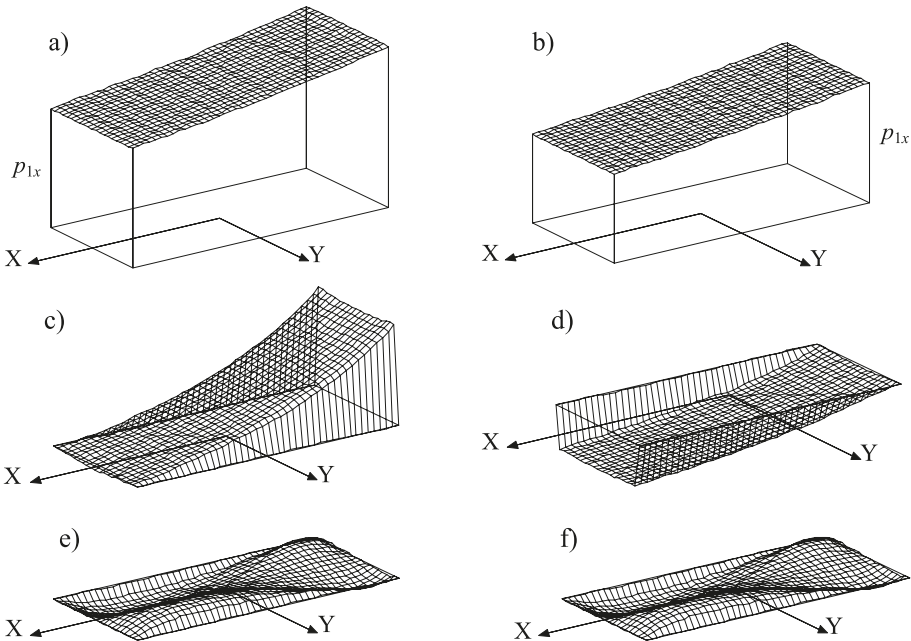
Fig. 9. The stresses in the adherends of a scarf joint loaded axially in the case of different materials: a) stress σ_{1x} (values × 1), b) stress σ_{2x} (values × 1), c) stress σ_{1y} (values × 100), d) stress σ_{2y} (values × 100), e) stress τ_{1xy} (values × 1000), f) stress τ_{2xy} (values × 1000)
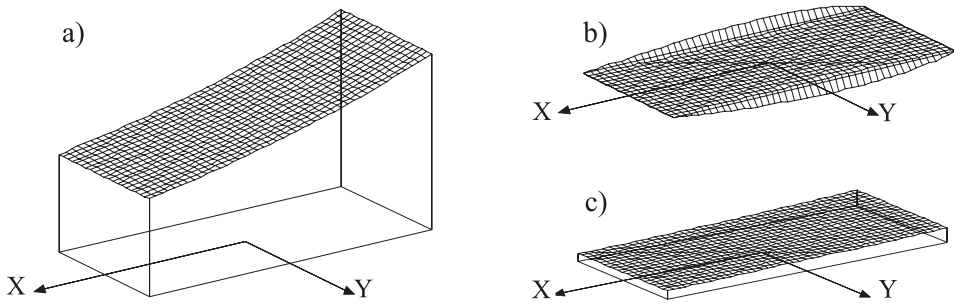
Fig. 10. The stresses in the adhesive of a scarf joint loaded axially in the case of different materials: a) stress τ_x (values × 10), b) stress τ_y (values × 10), c) stress σ_N (values × 10)

A scarf joint loaded by a bending moment

Let us now consider a scarf joint loaded by the bending moments $M_1 = -M_2 = M = 1$ N·cm resulting from the linearly distributed stresses on the edge $x = l_x$ of adherend 1 and on the edge $x = -l_x$ of adherend 2 (fig. 11). The dimensions, the material parameters and the finite difference mesh are assumed identical to the previously considered case of a scarf joint loaded axially. The kinematic boundary conditions are imposed on adherend 1 by constraining its node $(i, j) = (11, 23)$ in the direction of the X axis and the nodes $(i, j) = (11, 13)$, $(11, 33)$ in the direction of the Y axis.

Now a complete solution to the equations of the theory of elasticity will be presented. It will contain displacements and stresses in the adherends and in the adhesive.
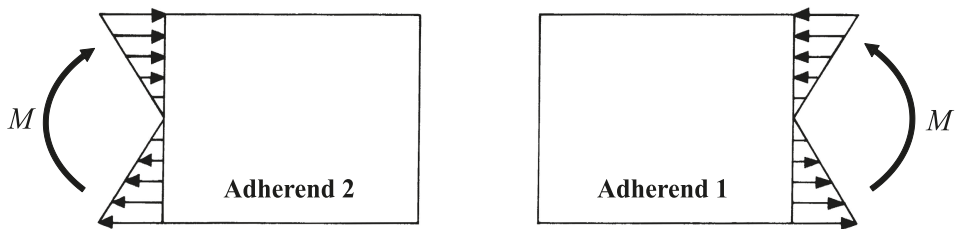
Fig. 11. Loading acting on the adherends of a scarf joint subjected to a bending moment

In the following, in the captions of the tables and figures presenting the complete solution, the flexibility of the adhesive is emphasized, to differentiate clearly from the case with an undeformable adhesive.

The distributions of displacement functions u_1, u_2 and v_1, v_2 for the adherends are given in fig. 12. The displacements for both adherends are depicted in single drawings, because with the adopted scale, the differences between the appropriate displacement values are indistinguishable.

a)

b)

Fig. 12. The displacements in adherends of a joint with a flexible adhesive loaded by the bending moment: a) displacements u_1, u_2, b) displacements v_1, v_2

The values of the adherend displacements at selected nodes of the finite difference mesh are given in table 2.

The values of stresses at selected points in adherends 1 and 2 of a joint with a flexible adhesive loaded by the moment are given in tables 3 and 4.

Table 2. The displacements in adherends of a joint with a flexible adhesive loaded by the bending moment [cm]

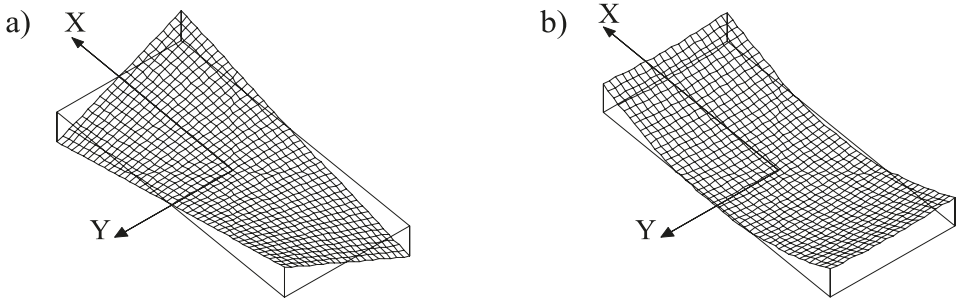|		Displacements of adherend 1					Displacements in adherend 2		
	$i \backslash j$	1	23	45		$i \backslash j$	1	23	45
u_1	1	$5.937 \cdot 10^{-8}$	$-1.646 \cdot 10^{-10}$	$-5.970 \cdot 10^{-8}$	u_2	1	$5.971 \cdot 10^{-8}$	$1.800 \cdot 10^{-10}$	$-5.935 \cdot 10^{-8}$
v_1		$5.840 \cdot 10^{-8}$	$-7.379 \cdot 10^{-9}$	$5.837 \cdot 10^{-8}$	v_2		$5.840 \cdot 10^{-8}$	$-7.379 \cdot 10^{-9}$	$5.837 \cdot 10^{-8}$
u_1	11	0	0	0	u_2	11	0	0	0
v_1		$5.213 \cdot 10^{-8}$	$-1.346 \cdot 10^{-8}$	$5.209 \cdot 10^{-8}$	v_2		$5.213 \cdot 10^{-8}$	$-1.346 \cdot 10^{-8}$	$5.209 \cdot 10^{-8}$
u_1	21	$-5.937 \cdot 10^{-8}$	$1.646 \cdot 10^{-10}$	$5.97 \cdot 10^{-8}$	u_2	21	$-5.971 \cdot 10^{-8}$	$-1.800 \cdot 10^{-10}$	$5.935 \cdot 10^{-8}$
v_1		$5.840 \cdot 10^{-8}$	$-7.379 \cdot 10^{-9}$	$5.837 \cdot 10^{-8}$	v_2		$5.840 \cdot 10^{-8}$	$-7.379 \cdot 10^{-9}$	$5.837 \cdot 10^{-8}$

Table 3. The stresses in adherend 1 of a scarf joint with a flexible adhesive loaded by the bending moment [N/cm²]

		Stresses				
	$i \backslash j$	1	2	23	44	45
σ_x	1	$-3.166 \cdot 10^{-3}$	$-3.170 \cdot 10^{-3}$	$-3.175 \cdot 10^{-3}$	$-3.170 \cdot 10^{-3}$	$-3.173 \cdot 10^{-3}$
σ_y		0	0	0	0	0
τ_{xy}		0	0	0	0	0
σ_x	2	$-2.856 \cdot 10^{-3}$	$-2.856 \cdot 10^{-3}$	$-2.857 \cdot 10^{-3}$	$-2.856 \cdot 10^{-3}$	$-2.855 \cdot 10^{-3}$
σ_y		$3.686 \cdot 10^{-6}$	$2.275 \cdot 10^{-6}$	$-1.722 \cdot 10^{-7}$	$2.263 \cdot 10^{-6}$	$3.709 \cdot 10^{-6}$
τ_{xy}		$-2.436 \cdot 10^{-6}$	$-2.940 \cdot 10^{-6}$	$-9.586 \cdot 10^{-7}$	$9.203 \cdot 10^{-7}$	0
σ_x	11	0	0	0	0	0
σ_y		0	0	0	0	0
τ_{xy}		$-1.954 \cdot 10^{-6}$	$-2.032 \cdot 10^{-6}$	$-1.020 \cdot 10^{-6}$	$-9.308E-9$	0

Table 3. Continued

	$i\backslash j$	1	2	23	44	45
σ_x	20	$2.856\cdot10^{-3}$	$2.856\cdot10^{-3}$	$2.857\cdot10^{-3}$	$2.856\cdot10^{-3}$	$2.855\cdot10^{-3}$
σ_y		$-3.686\cdot10^{-6}$	$-2.275\cdot10^{-6}$	$1.722\cdot10^{-7}$	$-2.263\cdot10^{-6}$	$-3.709\cdot10^{-6}$
τ_{xy}		$-2.436\cdot10^{-6}$	$-2.940\cdot10^{-6}$	$-9.586\cdot10^{-7}$	$9.203\cdot10^{-7}$	0
σ_x	21	$3.166\cdot10^{-3}$	$3.170\cdot10^{-3}$	$3.175\cdot10^{-3}$	$3.170\cdot10^{-3}$	$3.173\cdot10^{-3}$
σ_y		0	0	0	0	0
τ_{xy}		0	0	0	0	0

Table 4. The stresses in adherend 2 of a scarf joint with a flexible adhesive loaded by the bending moment [N/cm²]

Stresses						
	$i\backslash j$	1	2	23	44	45
σ_x	1	$-3.173\cdot10^{-3}$	$-3.170\cdot10^{-3}$	$-3.175\cdot10^{-3}$	$-3.170\cdot10^{-3}$	$-3.166\cdot10^{-3}$
σ_y		0	0	0	0	0
τ_{xy}		0	0	0	0	0
σ_x	2	$-2.855\cdot10^{-3}$	$-2.856\cdot10^{-3}$	$-2.857\cdot10^{-3}$	$-2.856\cdot10^{-3}$	$-2.856\cdot10^{-3}$
σ_y		$3.709\cdot10^{-6}$	$2.263\cdot10^{-6}$	$-1.722\cdot10^{-7}$	$2.275\cdot10^{-6}$	$3.686\cdot10^{-6}$
τ_{xy}		0	$-9.203\cdot10^{-7}$	$9.586\cdot10^{-7}$	$2.940\cdot10^{-6}$	$2.436\cdot10^{-6}$
σ_x	11	0	0	0	0	0
σ_y		0	0	0	0	0
τ_{xy}		0	$9.044\cdot10^{-9}$	$1.020\cdot10^{-6}$	$2.032\cdot10^{-6}$	$1.954\cdot10^{-6}$
σ_x	20	$2.855\cdot10^{-3}$	$2.856\cdot10^{-3}$	$2.857\cdot10^{-3}$	$2.856\cdot10^{-3}$	$2.856\cdot10^{-3}$
σ_y		$-3.709\cdot10^{-6}$	$-2.263\cdot10^{-6}$	$1.722\cdot10^{-7}$	$-2.275\cdot10^{-6}$	$-3.686\cdot10^{-6}$
τ_{xy}		0	$-9.203\cdot10^{-7}$	$9.586\cdot10^{-7}$	$2.940\cdot10^{-6}$	$2.436\cdot10^{-6}$
σ_x	21	$3.173\cdot10^{-3}$	$3.170\cdot10^{-3}$	$3.175\cdot10^{-3}$	$3.170\cdot10^{-3}$	$3.166\cdot10^{-3}$
σ_y		0	0	0	0	0
τ_{xy}		0	0	0	0	0

Table 5. The stresses in the flexible adhesive of a joint loaded by the bending moment [N/cm²]

Stresses				
	$i\backslash j$	1	23	45
τ_x	1	$-3.132\cdot10^{-4}$	$-3.105\cdot10^{-4}$	$-3.132\cdot10^{-4}$
τ_y		$-3.240\cdot10^{-7}$	0	$3.240\cdot10^{-7}$
σ_N		$-3.132\cdot10^{-5}$	$-3.105\cdot10^{-5}$	$-3.132\cdot10^{-5}$
τ_x	11	0	0	0
τ_y		$-2.031\cdot10^{-7}$	0	$2.031\cdot10^{-7}$
σ_N		0	0	0
τ_x	21	$3.132\cdot10^{-4}$	$3.105\cdot10^{-4}$	$3.132\cdot10^{-4}$
τ_y		$-3.240\cdot10^{-7}$	0	$3.240\cdot10^{-7}$
σ_N		$3.132\cdot10^{-5}$	$3.105\cdot10^{-5}$	$3.132\cdot10^{-5}$

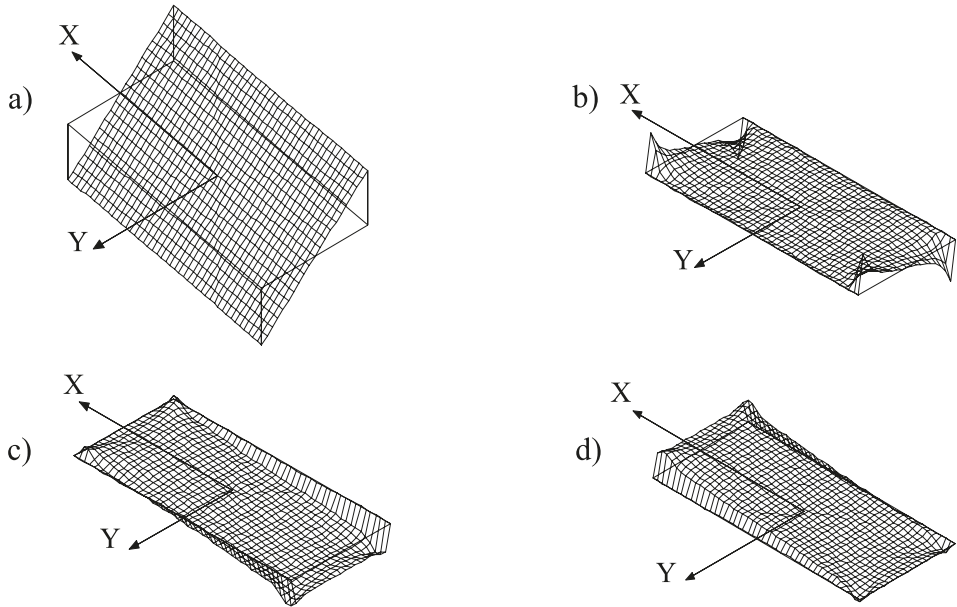The stress distributions in adherends 1 and 2 of a joint with a flexible adhesive are presented in fig. 13.

Fig. 13. The stresses in the adherends of a joint with a flexible adhesive loaded by the bending moment: a) stresses σ_{1x}, σ_{2x}, b) stresses σ_{1y}, σ_{2y} (values × 500), c) stress τ_{1xy} (values × 500), d) stress τ_{2xy} (values × 500)

The values of stresses in the flexible adhesive of a joint loaded by the moment are given in table 5, and the corresponding distributions – in fig. 14.
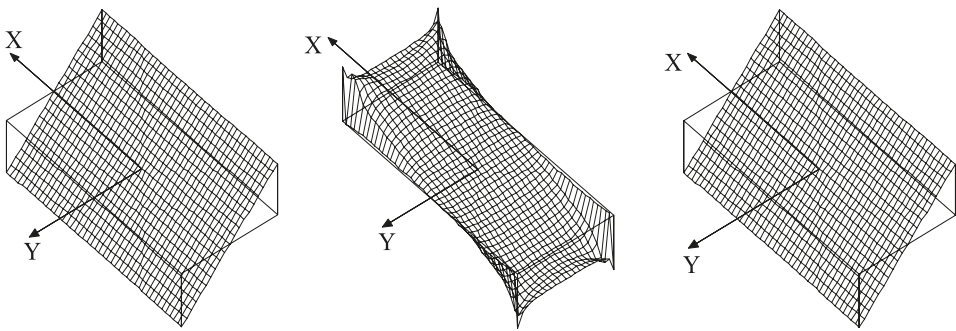
Fig. 14. The stresses in the flexible adhesive of a joint loaded by the bending moment: a) stress τ_x, b) stress τ_y (values × 1500), c) stress σ_N (values × 10)

In the adherends of the considered scarf joint, the normal stresses σ_{1x}, σ_{2x} dominate. They are equal to one another, constant along x and linear along y with an accuracy of 0.28%. The stress state in the adhesive itself is dominated by the shear

stresses τ_x and σ_N, which are also approximately constant along x and linear along y. Due to the adhesive flexibility $v_1 \neq v_2$. In this case, there are non-zero normal σ_{ky} and shear τ_{kxy} stresses (fig. 13b–d) in the adherends, and non-zero shear stress τ_y in the adhesive (fig. 14b). However, the stresses σ_{ky} and τ_{kxy} in the adherends are approx. 1000 times smaller than the stress σ_{kx}, and the stress τ_y in the adhesive is approx. 1500 times smaller than the stress τ_x. Hence, it can be assumed with sufficient accuracy that the stress states in the adherends of a joint with a flexible adhesive loaded by the bending moment M, are identical to the one in a continuous element subjected to the moment M. For $M = 1$ N·cm the outermost normal stress in the cross-section $g \times 2l_y$ of the continuous beam is $\sigma_x = \pm 3.173 \cdot 10^{-3}$ N/cm². These values differ by approx. 0.28% from the outermost stresses σ_{1x}, σ_{2x} in the adherends of a joint with a flexible adhesive (tables 3 and 4).

If the adhesive flexibility decreases, then the difference between the adherend displacements decreases, too. In the limiting case, for the undeformable adhesive, a physical interpretation ensures the equality of these displacements. This conclusion can be drawn from equations (22) – (25), too. Indeed, when one divides these equations by G_s and lets $G_s \rightarrow \infty$, then the identities $u_1 = u_2$ and $v_1 = v_2$ result. Thus, it may be assumed, that in the limiting case, the values and the distributions of stresses in the adherends of a scarf joint are identical, as in the continuous beam loaded by the bending moment M. If we denote these stresses by σ_x, σ_y, τ_{xy}, then we may write down:

$$\sigma_x(x, y) = -\frac{3M\,y}{2gl_y^3} \tag{51}$$

$$\sigma_y(x, y) = 0 \tag{52}$$

$$\tau_{xy} = 0 \tag{53}$$

Thus, the continuous element may serve as an approximate model of a scarf joint with a flexible adhesive. Indeed, it can be considered as a scarf joint with an undeformable adhesive. The undeformable adhesive is represented be a skew section in the continuous element. That skew section is oriented in the continuous element in the same way as the flexible adhesive in the scarf joint.

The displacements $u = u_1 = u_2$ and $v = v_1 = v_2$ of the continuous element with an undeformable adhesive fulfill the following set of equations:

$$\frac{E_x}{1 - v_{xy} v_{yx}} \frac{\partial u}{\partial x} + \frac{v_{xy} E_x}{1 - v_{xy} v_{yx}} \frac{\partial v}{\partial y} = -\frac{3M\,y}{2gl_y^3} \tag{54}$$

$$\frac{v_{yx}E_y}{1-v_{xy}v_{yx}}\frac{\partial u}{\partial x}+\frac{E_y}{1-v_{xy}v_{yx}}\frac{\partial v}{\partial y}=0 \tag{55}$$

$$\frac{\partial u}{\partial y}+\frac{\partial v}{\partial x}=0 \tag{56}$$

which results from substitution of the formulae (51) – (53) to the constitutive equations (16) – (18) in the case of the material properties E_x, E_y, G_{xy}, v_{xy}, v_{yx}.

Solving the equations (54) and (56) with respect to u and v, one gets:

$$u(x,y)=u_1(x,y)=u_2(x,y)=-\frac{3Mxy}{2E_xgl_y^3}-Ay+B \tag{57}$$

$$v(x,y)=v_1(x,y)=v_2(x,y)=\frac{3M(x^2+v_{yx}y^2)}{4E_xgl_y^3}+Ax+C \tag{58}$$

where: A, B, and C are arbitrary constants.

In the case of $G_s=\infty$, the functions u_1, u_2, v_1, v_2 presented above fulfill the equations (22) – (25) and the boundary conditions (29) – (36).

The constants A, B, and C follow from the kinematic boundary conditions, which can be expressed in co-ordinates as:
  – node $(i,j)=(11,23)$, co-ordinates $x=0$ and $y=0\rightarrow u(0,0)=0$
  – node $(i,j)=(11,13)$, co-ordinates $x=-x_0$ and $y=0\rightarrow v(-x_0,0)=0$
  – node $(i,j)=(21,33)$, co-ordinates $x=x_0$ and $y=0\rightarrow v(x_0,0)=0$,
where: $x_0=10.2(27)$ cm.

These conditions lead to $A=0$, $B=0$ and

$$C=-\frac{3Mx_0^2}{4E_xgl_y^3} \tag{59}$$

The displacements in the continuous element loaded by the bending moment, calculated from (57) – (59) are given in table 6. Comparison of the values presented in Tables 2 and 6 makes it possible to assess that the maximal displacements u_1, u_2 of the adherends of the joint with the flexible adhesive and the maximal displacement u of the continuous element are equal, with an accuracy of approx. 0.35%. Similarly, it can be assessed that the maximal displacements v_1, v_2 of the adherends of the joint with the flexible adhesive and the maximal displacement v of the continuous element are equal with an accuracy of approx. 0.85%.

Table 6. The displacements of the continuous element loaded by the bending moment [cm]

Displacements				
	$i \backslash j$	1	23	45
u	1	$5.949 \cdot 10^{-8}$	0	$-5.949 \cdot 10^{-8}$
v		$5.790 \cdot 10^{-8}$	$-7.393 \cdot 10^{-9}$	$5.790 \cdot 10^{-8}$
u	11	0	0	0
v		$5.180 \cdot 10^{-8}$	$-1.349 \cdot 10^{-8}$	$5.180 \cdot 10^{-8}$
u	21	$-5.949 \cdot 10^{-8}$	0	$5.949 \cdot 10^{-8}$
v		$5.790 \cdot 10^{-8}$	$-7.393 \cdot 10^{-9}$	$5.790 \cdot 10^{-8}$

Normal and shear stresses are present in the continuous element – in the skew section defined by the adhesive plane. However, in the limiting case $G_s = \infty$, the shear stresses in the skew section (undeformable adhesive) cannot be determined from the formulae (19) – (20) because in the view of $u_1 - u_2 = 0$, $v_1 - v_2 = 0$ and $G_s = \infty$, indeterminate symbols of the form $\infty \cdot 0$ are found. The shear stresses in the undeformable adhesive can be calculated from the equations (22) – (25), which do not explicitly include the differences of the displacements $u_1 - u_2$, $v_1 - v_2$ and the value G_s. If we determine $u_1 - u_2$, $v_1 - v_2$ from the formulae (19) – (20) and substitute them to (22) – (25), then for the parameters E_x, E_y, G_{xy}, v_{xy}, v_{yx} the following relations follow:

$$\left(\alpha_x \frac{\partial^2 u_1}{\partial x^2} + \frac{\partial^2 u_1}{\partial y^2} + \beta_x \frac{\partial^2 v_1}{\partial x \partial y} \right)\left(\frac{g}{2l_x} x + \frac{g}{2} \right) + \left(\alpha_x \frac{\partial u_1}{\partial x} + (\beta_x - 1)\frac{\partial v_1}{\partial y} \right)\frac{g}{2l_x} - \frac{\tau_x}{G_{xy} \cos^2 \varphi_x} = 0 \quad (60)$$

$$\left(\frac{\partial^2 v_1}{\partial x^2} + \alpha_y \frac{\partial^2 v_1}{\partial y^2} + \beta_y \frac{\partial^2 u_1}{\partial x \partial y} \right)\left(\frac{g}{2l_x} x + \frac{g}{2} \right) + \left(\frac{\partial u_1}{\partial y} + \frac{\partial v_1}{\partial x} \right)\frac{g}{2l_x} - \frac{\tau_y}{G_{xy} \cos \varphi_x} = 0 \quad (61)$$

$$\left(\alpha_x \frac{\partial^2 u_2}{\partial x^2} + \frac{\partial^2 u_2}{\partial y^2} + \beta_x \frac{\partial^2 v_2}{\partial x \partial y} \right)\left(-\frac{g}{2l_x} x + \frac{g}{2} \right) - \left(\alpha_x \frac{\partial u_2}{\partial x} + (\beta_x - 1)\frac{\partial v_2}{\partial y} \right)\frac{g}{2l_x} + \frac{\tau_x}{G_{xy} \cos^2 \varphi_x} = 0 \quad (62)$$

$$\left(\frac{\partial^2 v_2}{\partial x^2} + \alpha_y \frac{\partial^2 v_2}{\partial y^2} + \beta_y \frac{\partial^2 u_2}{\partial x \partial y} \right)\left(-\frac{g}{2l_x} x + \frac{g}{2} \right) - \left(\frac{\partial u_2}{\partial y} + \frac{\partial v_2}{\partial x} \right)\frac{g}{2l_x} + \frac{\tau_y}{G_{xy} \cos \varphi_x} = 0 \quad (63)$$

where:

$$\alpha_x = \frac{E_x}{G_{xy}(1 - v_{xy} v_{yx})}, \quad \alpha_y = \frac{E_y}{G_{xy}(1 - v_{xy} v_{yx})} \quad (64)$$

$$\beta_x = 1 + \frac{v_{xy}E_x}{G_{xy}(1-v_{xy}v_{yx})} = 1 + \alpha_x v_{xy}, \quad \beta_y = 1 + \frac{v_{yx}E_y}{G_{xy}(1-v_{xy}v_{yx})} = 1 + \alpha_y v_{yx} \qquad (65)$$

Substitution of the functions u_1, u_2, v_1, and v_2 given in (57) – (59) to the equations (60) and (61) or (62) and (63) leads to the relations defining the stresses in the undeformable adhesive in the continuous element:

$$\tau_x(x,y) = \sigma_x(x,y)\sin\varphi_x\cos\varphi_x \qquad (66)$$

$$\tau_y(x,y) = 0 \qquad (67)$$

where: $\sigma_x(x,y)$ is given by (51).

The formulae (21) and (66) yield the relation for the normal stress in the undeformable adhesive:

$$\sigma_N(x,y) = \sigma_x(x,y)\sin^2\varphi_x \qquad (68)$$

The formulae (66) – (68) can also be derived in an elementary manner, considering the equilibrium conditions of the adherend in the vicinity of the adhesive. The stresses values for the undeformable adhesive in the continuous element following from (66) – (68) are given in table 7.

Table 7. The stresses for the undeformable adhesive in the continuous element loaded by the bending moment [N/cm²]

Stresses				
	$i \backslash j$	1	23	45
τ_x		$-3.141\cdot10^{-4}$	$-3.141\cdot10^{-4}$	$-3.141\cdot10^{-4}$
τ_y	1	0	0	0
σ_N		$-3.141\cdot10^{-5}$	$-3.141\cdot10^{-5}$	$-3.141\cdot10^{-5}$
τ_x		0	0	0
τ_y	11	0	0	0
σ_N		0	0	0
τ_x		$3.141\cdot10^{-4}$	$3.141\cdot10^{-4}$	$3.141\cdot10^{-4}$
τ_y	21	0	0	0
σ_N		$3.141\cdot10^{-5}$	$3.141\cdot10^{-5}$	$3.141\cdot10^{-5}$

Comparison of the values given in tables 5 and 7 makes it possible to assess with an accuracy of approx. 0.3% that the maximal stresses in the flexible adhesive and in the undeformable adhesive in the continuous element are equal.

It can be concluded that the values and distributions of the displacements and stresses in the considered case of the scarf joint with the flexible adhesive are

similar to those in the case of the continuous plane stress element (in the scarf joint with the undeformable adhesive) subjected to the bending moment in the plane 0XY. The smaller is the adhesive flexibility, the better the approximation.

A scarf joint loaded by a shear force

The way in which a shear force is transmitted through a scarf joint can be illustrated, when the force is constant along the joint. Let us assume that adherend 1 is subjected to the shear force $-T$ at the edge $x = l_x$, and adherend 2 – to the shear force T at the edge $x = -l_x$. The joint loaded in this way has to be equilibrated, e.g. by additional bending moments $M = T \cdot l_x$, according to fig. 15a.
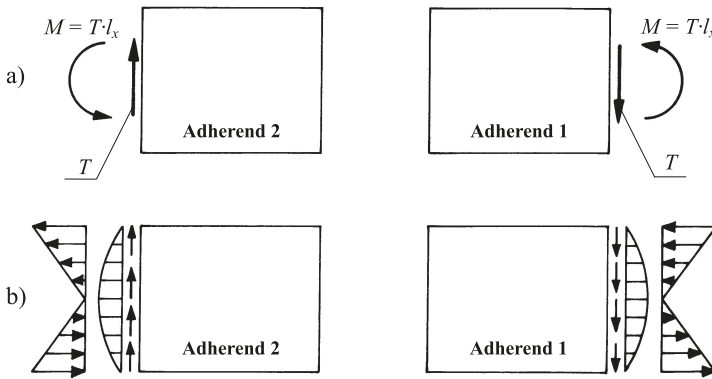
Fig. 15. A scarf joint subjected to a shear force and a bending moment

In the following, the load of $T = 1.0$ N is assumed in the form of a parabolic distributed shear stress, and the bending moment $M = T l_x$ in the form of a linearly distributed normal stress (fig. 15b). All the remaining data are the same as in the previous case of the joint loaded by the bending moment.

The distributions and values of the displacements u_1, u_2, v_1, and v_2 for a scarf joint with a flexible adhesive are presented in fig. 16 and in table 8.

Fig. 16. The displacements in adherends of a joint with a flexible adhesive loaded by the shear force and the bending moment: a) displacements u_1, u_2, b) displacements v_1, v_2

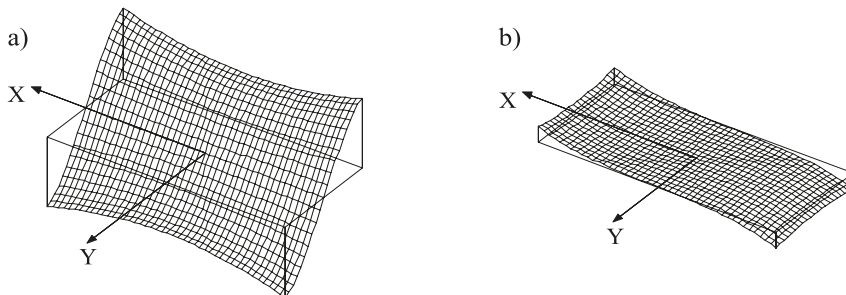**Table 8. The displacements in adherends of a joint with a flexible adhesive loaded by the shear force and the bending moment [cm]**

		Displacements in adherend 1				Displacements in adherend 2		
	$i\backslash j$	1	23	45	$i\backslash j$	1	23	45
u_1	1	$-2.507 \cdot 10^{-6}$	$-1.841 \cdot 10^{-6}$	$-2.514 \cdot 10^{-6}$	u_2	1	$-2.514 \cdot 10^{-6}$	$-1.841 \cdot 10^{-6}$	$-2.507 \cdot 10^{-6}$
v_1		$-5.666 \cdot 10^{-7}$	$2.178 \cdot 10^{-10}$	$5.671 \cdot 10^{-7}$	v_2		$-5.667 \cdot 10^{-7}$	$2.479 \cdot 10^{-10}$	$5.671 \cdot 10^{-7}$
u_1	11	0	0	0	u_2	11	0	0	0
v_1		$-4.081 \cdot 10^{-7}$	$-6.661 \cdot 10^{-10}$	$4.068 \cdot 10^{-7}$	v_2		$-4.063 \cdot 10^{-7}$	$1.13 \cdot 10^{-9}$	$4.086 \cdot 10^{-7}$
u_1	21	$2.507 \cdot 10^{-6}$	$1.841 \cdot 10^{-6}$	$2.514 \cdot 10^{-6}$	u_2	21	$2.514 \cdot 10^{-6}$	$1.841 \cdot 10^{-6}$	$2.507 \cdot 10^{-6}$
v_1		$-5.666 \cdot 10^{-7}$	$2.178 \cdot 10^{-10}$	$5.671 \cdot 10^{-7}$	v_2		$-5.667 \cdot 10^{-7}$	$2.479 \cdot 10^{-10}$	$5.671 \cdot 10^{-7}$

The distributions of stresses in the adherends of a scarf joint with a flexible adhesive loaded by the shear force and the bending moment are presented in fig. 17. The particular stresses are represented in single figures, because the differences between their values for both adherends are negligible and indistinguishable with the adopted scale.
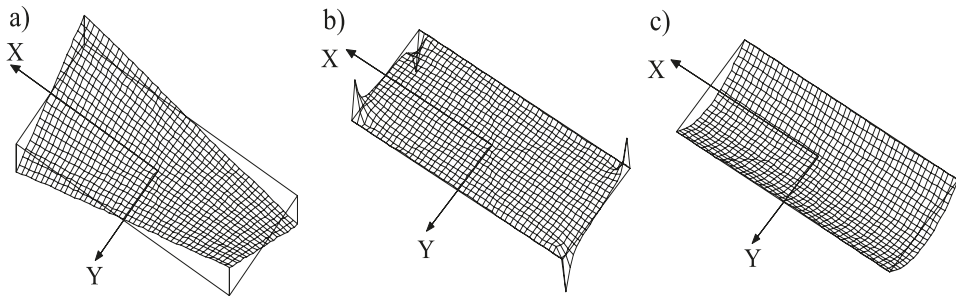

Fig. 17. The stresses in the adherends of a scarf joint with a flexible adhesive loaded by the shear force and the bending moment: a) stresses σ_{1x}, σ_{1x}, b) stresses σ_{1y}, σ_{1y} (values × 100), c) stresses τ_{1xy}, τ_{1xy}

The values of the stresses in the adherends of a scarf joint with a flexible adhesive loaded by the shear force and the bending moment are given in table 9.

Table 9. The stresses in the adherends of a scarf joint with a flexible adhesive loaded by the shear force and the bending moment [N/cm²]

		Adherend 1				Adherend 2		
	$i\backslash j$	1	23	45		1	23	45
σ_x	1	$7.034 \cdot 10^{-2}$	$-2.059 \cdot 10^{-4}$	$-7.139 \cdot 10^{-2}$	σ_x	$7.139 \cdot 10^{-2}$	$2.060 \cdot 10^{-4}$	$-7.034 \cdot 10^{-2}$
σ_y		0	0	0	σ_y	0	0	0
τ_{xy}		0	0	0	τ_{xy}	0	0	0

Table 9. Continued

	$i\backslash j$	1	23	45		1	23	45
σ_x		$6.338\cdot10^{-2}$	$-1.842\cdot10^{-4}$	$-6.425\cdot10^{-2}$	σ_x	$6.425\cdot10^{-2}$	$1.843\cdot10^{-4}$	$-6.338\cdot10^{-2}$
σ_y	2	$-6.312\cdot10^{-4}$	$6.539\cdot10^{-6}$	$6.329\cdot10^{-4}$	σ_y	$-6.329\cdot10^{-4}$	$-6.522\cdot10^{-6}$	$6.312\cdot10^{-4}$
τ_{xy}		$-2.810\cdot10^{-3}$	$-3.090\cdot10^{-3}$	$-3.089\cdot10^{-3}$	τ_{xy}	$-3.089\cdot10^{-3}$	$-3.090\cdot10^{-3}$	$-2.810\cdot10^{-3}$
σ_x		0	0	0	σ_x	0	0	0
σ_y	11	0	0	0	σ_y	0	0	0
τ_{xy}		$-1.623\cdot10^{-2}$	$-1.624\cdot10^{-2}$	$-1.626\cdot10^{-2}$	τ_{xy}	$-1.626\cdot10^{-2}$	$-1.624\cdot10^{-2}$	$-1.623\cdot10^{-2}$
σ_x		$-6.338\cdot10^{-2}$	$1.842\cdot10^{-4}$	$6.425\cdot10^{-2}$	σ_x	$-6.425\cdot10^{-2}$	$-1.843\cdot10^{-4}$	$6.338\cdot10^{-2}$
σ_y	20	$6.312\cdot10^{-4}$	$-6.539\cdot10^{-6}$	$-6.329\cdot10^{-4}$	σ_y	$6.329\cdot10^{-4}$	$6.522\cdot10^{-6}$	$-6.312\cdot10^{-4}$
τ_{xy}		$-2.810\cdot10^{-3}$	$-3.090\cdot10^{-3}$	$-3.089\cdot10^{-3}$	τ_{xy}	$-3.089\cdot10^{-3}$	$-3.090\cdot10^{-3}$	$-2.810\cdot10^{-3}$
σ_x		$-7.034\cdot10^{-2}$	$2.059\cdot10^{-4}$	$7.139\cdot10^{-2}$	σ_x	$-7.139\cdot10^{-2}$	$-2.060\cdot10^{-4}$	$7.034\cdot10^{-2}$
σ_y	21	0	0	0	σ_y	0	0	0
τ_{xy}		0	0	0	τ_{xy}	0	0	0

The values of the stresses in the flexible adhesive of a scarf joint loaded by the shear force and the bending moment are presented in table 10, and the corresponding distributions – in fig. 18.

Table 10. The stresses in the flexible adhesive of a scarf joint loaded by the shear force and the bending moment [N/cm²]

			Stresses	
	$i\backslash j$	1	23	45
τ_x		$6.917\cdot10^{-3}$	0	$-6.917\cdot10^{-3}$
τ_y	1	$6.784\cdot10^{-5}$	$-2.707\cdot10^{-5}$	$6.784\cdot10^{-5}$
σ_N		$6.917\cdot10^{-4}$	0	$-6.917\cdot10^{-4}$
τ_x		0	0	0
τ_y	11	$-1.614\cdot10^{-3}$	$-1.617\cdot10^{-3}$	$-1.614\cdot10^{-3}$
σ_N		0	0	0
τ_x		$-6.917\cdot10^{-3}$	0	$6.917\cdot10^{-3}$
τ_y	21	$6.784\cdot10^{-5}$	$-2.707\cdot10^{-5}$	$6.784\cdot10^{-5}$
σ_N		$-6.917\cdot10^{-4}$	0	$6.917\cdot10^{-4}$

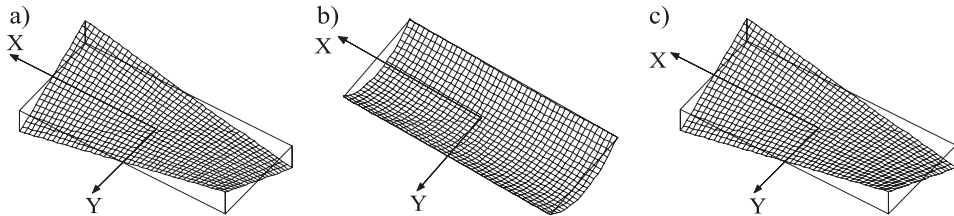**Fig. 18. The stresses in the flexible adhesive of a scarf joint loaded by the shear force and the bending moment: a) stress τ_x, b) stress τ_y, c) stress σ_N (values × 10)**

Comparison of figs. 17a, b and figs. 13 a, b leads to the conclusion that the normal stresses σ_{kx} and σ_{ky} shown in figs. 17a and b result from the bending moment $M = Tl_x$, while the shear stresses τ_{kxy} are due to the action of the shear force T only. Thus, the action of the shear force can be separated, and in this way, how the joint transmits the shear force can be assessed.

As in the case of the joint loaded by the bending moment, in the scarf joint with the flexible adhesive loaded by the shear force and the bending moment, the distribution of the stresses in the adherends are similar to those in the case of the continuous plane stress element (in the joint with the undeformable adhesive). The stresses σ_x, σ_y, and τ_{xy} in the adherends of the joint with the undeformable adhesive can be given by the following formulae:

$$\sigma_x(x,y) = \sigma_{kx}(x,y) = -\frac{3Txy}{2gl_y^3} \tag{69}$$

$$\sigma_y(x,y) = \sigma_{ky}(x,y) = 0 \tag{70}$$

$$\tau_{xy} = \tau_{kxy}(x,y) = -\frac{3T(l_y^2 - y^2)}{4gl_y^3} \tag{71}$$

The displacements $u = u_1 = u_2$ and $v = v_1 = v_2$ of the continuous element with the undeformable adhesive fulfill the set of equations:

$$\frac{E_x}{1 - v_{xy}v_{yx}} \frac{\partial u}{\partial x} + \frac{v_{xy}E_x}{1 - v_{xy}v_{yx}} \frac{\partial v}{\partial y} = -\frac{3Txy}{2gl_y^3} \tag{72}$$

$$\frac{v_{yx}E_y}{1 - v_{xy}v_{yx}} \frac{\partial u}{\partial x} + \frac{E_y}{1 - v_{xy}v_{yx}} \frac{\partial v}{\partial y} = 0 \tag{73}$$

$$\frac{\partial u}{\partial y} + \frac{\partial v}{\partial x} = -\frac{3T(l_y^2 - y^2)}{4G_{xy}gl_y^3} \tag{74}$$

which results from substitution of the relations (69) – (71) to the constitutive equations (16) – (18) for the material parameters E_x, E_y, G_{xy}, v_{xy}, v_{yx}. Equations (72) – (74) can be solved in a similar way to equations (54) – (56) to get:

$$u(x,y) = u_1(x,y) = u_2(x,y) = -\frac{3Tx^2y}{4E_xgl_y^3} - \frac{3Tl_y^2y}{4G_{xy}gl_y^3} + \frac{Ty^3}{4G_{xy}gl_y^3} - \frac{Tv_{yx}y^3}{4E_xgl_y^3} - Ay + B \tag{75}$$

$$\upsilon(x, y) = \upsilon_1(x, y) = \upsilon_2(x, y) = \frac{3Tv_{yx}xy^2}{4E_xgl_y^3} + \frac{Tx^3}{4E_xgl_y^3} + Ax + C \qquad (76)$$

where: A, B, C are arbitrary constants.

For the undeformable adhesive ($G_s = \infty$) and the displacements u_1, u_2, v_1, and v_2 given by (75) and (76), equations (22) – (25) and the boundary conditions (29) – (36) are fulfilled as identities.

The kinematic boundary conditions expressed in the co-ordinates take the same form as in the previous example:

$$u(0, 0) = 0, \quad \upsilon(-x_0, 0) = 0, \quad \upsilon(x_0, 0) = 0,$$

where $x_0 = 10.2(27)$ cm. They yield $B = 0$, $C = 0$ and

$$A = \frac{Tx_0^2}{4E_xgl_y^3} \qquad (77)$$

The displacements of the continuous element loaded by the shear force and the bending moment resulting from (75) – (77) are given in table 11.

Comparison of the values given in tables 8 and 11 makes it possible to assess that the maximal displacements u_1 and u_2 of the adherends of the joint with the flexible adhesive and the maximal displacement u of the continuous element coincide with an accuracy of approx. 0.8%. Similarly, it can be assessed that the maximal displacements v_1, v_2 of the adherends of the joint with the flexible adhesive and the maximal displacement v of the continuous element, coincide with an accuracy of approx. 7.3%. It should be noted, that the displacements v_1, v_2, and v are about 5 times smaller than the displacements u_1, u_2, and u.

Table 11. The displacements in the continuous element loaded by the shear force and the bending moment [cm]

		Displacements		
	$i\backslash j$	1	23	45
u	1	$-2.496 \cdot 10^{-6}$	$-1.877 \cdot 10^{-6}$	$-2.496 \cdot 10^{-6}$
υ		$-5.257 \cdot 10^{-7}$	0	$5.257 \cdot 10^{-7}$
u	11	0	0	0
υ		$-3.885 \cdot 10^{-7}$	0	$3.885 \cdot 10^{-7}$
u	21	$2.496 \cdot 10^{-6}$	$1.877 \cdot 10^{-6}$	$2.496 \cdot 10^{-6}$
υ		$-5.257 \cdot 10^{-7}$	0	$5.257 \cdot 10^{-7}$

Substitution of the functions given by (75) and (76) to the equations (60) and (61) or (62) and (63) leads the formulae for the shear stresses in the undefor-

mable adhesive for the continuous element loaded by the shear force and the moment:

$$\tau_x(x, y) = \sigma_x(x, y)\sin\varphi_x\cos\varphi_x \qquad (78)$$

$$\tau_y(x, y) = \tau_{xy}(x, y)\sin\varphi_x \qquad (79)$$

The relations (21) and (78) lead to the expression for the normal stress in the undeformable adhesive:

$$\sigma_N(x, y) = \sigma_x(x, y)\sin^2\varphi_x \qquad (80)$$

The stresses in the undeformable adhesive of the continuous element loaded by the shear force and the bending moment are presented in table 12.

Comparison of the values in tables 10 and 12 makes it possible to assess that the maximal stresses in the flexible adhesive of the scarf joint loaded by the shear force and the bending moment, and the maximal stresses in the undeformable adhesive in the continuous element loaded likewise, coincide with an accuracy of approx. 2% in the case of τ_x and σ_N, and approx. 0.25% in the case of τ_y.

Table 12. The stresses in the undeformable adhesive of the continuous element loaded by the shear force and the bending moment [N/cm²]

			Stresses		
		$i\backslash j$	1	23	45
τ_x			$7.068\cdot10^{-3}$	0	$-7.068\cdot10^{-3}$
τ_y	1		0	0	0
σ_N			$7.068\cdot10^{-4}$	0	$-7.068\cdot10^{-4}$
τ_x			0	0	0
τ_y	11		$-1.618\cdot10^{-3}$	$-1.618\cdot10^{-3}$	$-1.618\cdot10^{-3}$
σ_N			0	0	0
τ_x			$-7.068\cdot10^{-3}$	0	$7.068\cdot10^{-3}$
τ_y	21		0	0	0
σ_N			$-7.068\cdot10^{-4}$	0	$7.068\cdot10^{-4}$

The calculations carried out lead to the conclusion that the considered scarf joint with the flexible adhesive loaded by the shear force and the bending moment, features the values of the displacements and the distributions of stresses in the adhesive and the adherends similar to those in the continuous plane stress element (in the joint with the undeformable adhesive) loaded likewise. In particular, the distributions of the stresses τ_{kxy} in the adherends and the stress τ_y in the adhesive due to the action of the shear force are parabolic with an accuracy of approx. 0.25%. The smaller is the adhesive flexibility, the better the approximation.

Conclusions

In a scarf joint loaded axially, where both adherends are made of the same material, the stress states in the adherends and the adhesive do not depend on the adhesive thickness or its material parameters, and are identical to those in the continuous element under a uniaxial stress state. The adhesive parameters only influence the difference between the adherend displacements.

The equivalence of the one-dimensional and two-dimensional models, and the independence of values and distributions of stresses with respect to the adhesive parameters, do not exist when: a scarf joint is made of two different materials, adherends are not loaded uniformly and axially or in the case of adherends with differing thicknesses.

A general conclusion may be formulated that a scarf joint with an adhesive of little flexibility between two adherends made of the same material and of the same thickness, transmits axial forces, bending moments and shear forces in the same or in a similar way to a continuous element considered as the scarf joint with an imaginary undeformable adhesive.

In general, the smaller is the adhesive flexibility, the smaller the difference between the solution to the two-dimensional problem of the scarf joint with the flexible adhesive and the analytical solution to the joint with the undeformable adhesive. Thus, an approximate equivalence of displacements and stress states between an element made of two adherends with a scarf joint and the continuous element occurs.

This final statement is not obvious, because in a scarf joint loaded in the way discussed previously, the decreasing adhesive flexibility leads to a change in the nonlinear displacements and stress distributions in the adhesive to linear ones, corresponding to the continuous element considered as the scarf joint with an imaginary undeformable adhesive. On the other hand, in the joint with non-sharp edges, this behaviour is reversed – due to a decrease in the adhesive flexibility in the vicinity of the loaded edges, the stress concentrations are more pronounced and the displacement and stress distributions become increasingly non-linear.

References

Erdogan F., Ratawani M. [1971]: Stress Distribution in Bonded Joints. Journal of Composite Materials 5 (3): 378–393. DOI: 10.1177/002199837100500308

Goodman J.R., Bodig J. [1970]: Orthotropic Elastic Properties of Wood. Journal of the Structural Division 96 (11): 2301–2319

Keylwerth R. [1951]: Die anisotrope Elastzität des Holzes und der Lagerhölzer (Anisotropic elasticity of wood and wooden beams). VDI – Forschungsheft 430, Ausgabe 13, Band 17, Deuther Ingeniur, Dusseldorf

Neuhaus H. [1994]: Lehrbuch des Ingenieurholzbaus (Textbook on wood structures). Teubner, Stuttgart

Rapp P. [2010a]: Mechanika połączeń klejowych jako płaskie zadanie teorii sprężystości (Mechanics of adhesive joints as a plane problem of the theory of elasticity). Rozprawy Nr 441, Wydawnictwo Politechniki Poznańskiej, Poznań

Rapp P. [2010b]: Mechanics of adhesive joints as a plane problem of the theory of elasticity. Part I: general formulation. Archives of Civil and Mechanical Engineering 10 (2): 81–108

Reddy M.N., Sinha P.K. [1975]: Stresses in Adhesive-Bonded Joints for Composites. Fibre Science and Technology 8 (1): 33–47. DOI: 10.1016/0015-0568(75)90013-5

Smardzewski J. [1996]: Distribution of stresses in finger joints. Wood Science and Technology 30 (6): 477–489. DOI: 10.1007/BF00244442

Tomasiuk A. [1988]: Analyse der Spannungen in Klebfugen biegebelasteter Keilzinkenverbindungen (Analysis of stresses in scarf adhesive joints under bending). Holztechnologie – Leipzig 29 (1): 25–26